JOURNAL OF SPACECRAFT AND ROCKETS
Vol. 31, No. 4, July–August 1994

Atomic-Oxygen Undercutting of Long Duration Exposure Facility Aluminized-Kapton Multilayer Insulation

Kim K. de Groh* and Bruce A. Banks†
NASA Lewis Research Center, Cleveland, Ohio 44135

Atomic-oxygen undercutting is a potential threat to vulnerable spacecraft materials which have atomic-oxygen protective coatings. Such undercutting is due to the atomic-oxygen attack of oxidizable materials at microscopic defects in the protective coatings. These defects occur during fabrication and handling, or from micrometeoroid and debris bombardment in space. An aluminized-polyimide Kapton multilayer insulation sample that was located on the leading edge of the Long Duration Exposure Facility has been used to study low Earth orbit atomic-oxygen undercutting. Cracks in the aluminized coating located around vent holes provided excellent defect sites for the evaluation of atomic-oxygen undercutting. The experimentally observed undercut profiles were compared to predictions from Monte Carlo models for normal incident space ram atomic-oxygen attack. The shape of the undercut profile was found to vary with crack width, which is proportional to the number of oxygen atoms entering the crack. The resulting profiles of atomic-oxygen undercutting which occurred on the aluminized-Kapton sample indicated wide undercut cavities in spite of the fixed ram orientation. Potential causes of the observed undercutting are presented. Implications of the undercutting profiles relevant to Space Station Freedom are also discussed.

Nomenclature

$G(V)$ = Maxwell speed distribution function atoms, s/m
$\overline{V}$ = mean atomic-oxygen velocity, m/s
V_A = atmospheric velocity, m/s
V_m = most probable atomic-oxygen velocity, m/s
V_O = orbital velocity, m/s
V_R = ram atomic-oxygen velocity relative to spacecraft surface, m/s
V_{RM} = misaligned ram atomic-oxygen velocity due to thermal velocity contributions, m/s
V_{rms} = thermal velocity of average-energy atomic oxygen, m/s
θ = = maximum misalignment angle from ram for average-energy atomic oxygen
ϕ = angle of sweep of the ram velocity in LDEF's horizontal plane

Introduction

IN low Earth orbit (LEO) a harsh environment exists which can cause considerable damage to vulnerable spacecraft materials. The environment experienced by orbiting spacecraft includes atomic oxygen, ultraviolet radiation, thermal cycling, and micrometeoroid and debris bombardment.[1] Atomic oxygen, the predominant species in LEO,[2] has an average energy of ≈4.5 eV at ram impact velocities and is extremely reactive. Materials that are susceptible to oxidation must be protected when used for long durations in LEO. Atomic-oxygen attack of protected oxidizable materials can occur at microscopic pinhole defects (voids) or scratches in the protective coatings which are a result of fabrication and handling, or due to micrometeoroid and debris bombardment. At such defect sites, oxidation of underlying materials which have volatile oxidation products causes undercutting. Atomic-oxygen undercutting can produce cavities in the oxidized material which are larger than the original defects in the protective coating. Atomic-oxygen undercutting of protected polymers can result in the degradation of several materials' properties (i.e., mechanical, optical, etc.), which may affect system performance. Undercutting may also cause further damage to the protective coating if the protective coating tears or curls when undercut. This damage mechanism of undercutting and tearing may propagate and lead to structural failures.

Spacecraft materials which have shown a tendency to degrade (based on ground-laboratory atomic-oxygen evaluation) through an undercutting-tearing propagation mechanism include early configuration protected polyimide Kapton photovoltaic solar array blanket materials[3] and protected and reflective graphite epoxy solar concentrator materials[4] for Space Station Freedom. Other spacecraft materials that have the potential for degradation through undercutting include fiberglass epoxy composite structural members used for photovoltaic array extension and any oxidizable material shielded with a protective coating.

As a result of the potential damaging effects of atomic-oxygen undercutting, efforts have been made to understand and model the erosion processes that occur in various atomic-oxygen environments (normal incident space ram, sweeping (sun tracking) space ram, ground-based directed atomic oxygen, ground-based sweeping atomic oxygen, and plasma asher atomic-oxygen exposure). Monte Carlo models have been developed for protected polyimide Kapton substrates, based on ground-based undercut profiles at scratch sites, which predict atomic-oxygen undercut profiles for both space and ground-based atomic-oxygen environments.[5,6] Comparison of the Monte Carlo predicted LEO undercut profiles with actual space flight samples should contribute to the understanding of LEO materials durability and help to improve Monte Carlo predictions based on ground-laboratory testing.

The Long Duration Exposure Facility (LDEF) was in orbit for 5.8 years. This provided an excellent opportunity to study LEO direct ram atomic-oxygen undercutting. Undercutting of protected oxidizable materials at defect sites on ram facing surfaces was expected to occur on the LDEF (because of atomic-oxygen velocity components which are transverse to the ram

Received July 23, 1992; revision received July 25, 1993; accepted for publication July 27, 1993.

*Materials Research Engineer, Electro-Physics Branch, Power Technology Division, M.S. 309-2, 21000 Brookpark Road. Member AIAA.
†Chief, Electro-Physics Branch, Power Technology Division, M.S. 309-2, 21000 Brookpark Road.

direction), even though the LDEF was in a fixed orbital orientation.

Three causes of atomic-oxygen transverse velocity components have been identified which contribute to normal incident direct ram undercutting. The first of these causes involves the scattering of unreacted atomic oxygen. Upon entering a hole in the protective coating, atomic oxygen has a certain probability of reaction on first impact for a particular material (only ≈14% for Kapton[6]). The unreacted atomic oxygen is scattered approximately with a cosine distribution. Unreacted atomic oxygen scattered below the protective coating may have multiple opportunities to react with the substrate material, thus causing undercutting (see Fig. 1).

The second cause of undercutting involves the transverse velocity component of the thermal velocity of atomic oxygen. Atomic oxygen in LEO during the LDEF mission had an average temperature of 1227 K (Ref. 7). A Maxwellian distribution of speeds of the atomic oxygen existed, having random orientation which was vectorially added to the orbital ram velocity. The result is that atomic-oxygen impact velocities had a distribution of directions and energies. The thermal velocity of an average-energy oxygen atom V_{rms} for the LDEF altitudes was ≈1.4 km/s. The maximum misalignment from ram direction of an average-energy oxygen atom has been calculated to be ≈10 deg (see Fig. 2). An orbital velocity V_O of ≈7.7 km/s was used based on the LDEF's average atomic-oxygen fluence altitude (411 km). Thus, there was an angular distribution of atomic-oxygen flux impacting the LDEF due to thermal velocity contributions.

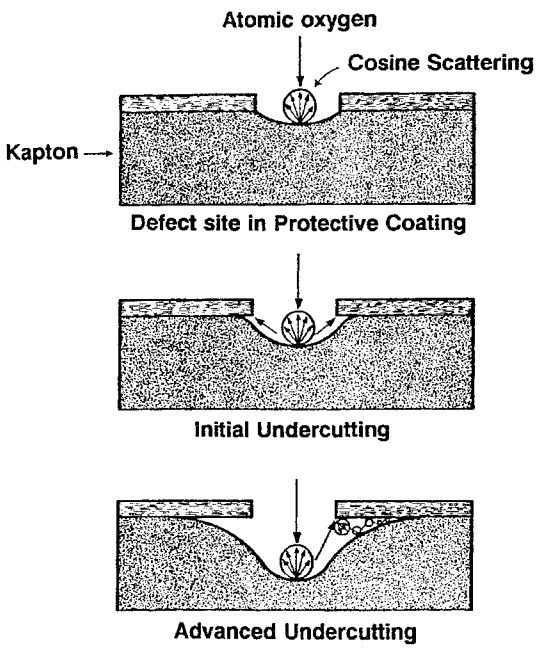

Fig. 1 Contribution to atomic-oxygen undercutting due to unreacted atomic oxygen scattered with a near cosine distribution.

The third cause of undercutting oxidation is the result of an additional transverse velocity component which occurred because the orbit of the LDEF was at an ≈28.5-deg inclination with respect to the Earth's atmospheric velocity vector. This caused the ram atomic-oxygen direction to sweep sinusoidally in the LDEF's horizontal plane. Figure 3 shows schematically how the ram atomic-oxygen direction varied by ≈3.7-deg. An atmospheric velocity at the LDEF orbit due to the Earth's rotation of 0.493 km/s, and an orbital velocity at 411 km of 7.673 km/s were used to calculate the 1.86-deg ram velocity sweep from the fixed orbital orientation.

As a result of the thermal and orbital inclination contributions, there was a Gaussian distribution of the time-averaged atomic-oxygen flux with respect to angle from the average velocity vector. Because of the orbital inclination, the angular flux distribution was wider in the LDEF's horizontal plane than in its vertical plane. This is shown schematically in Fig. 4. To visualize what effect the variation in flux distribution in the LDEF's horizontal and vertical planes can have on the LDEF materials, one can consider a pinhole camera containing an oxidizable material, located on the LDEF's leading edge. It would be expected that a slightly elliptical erosion region would occur, with the longest axis in the LDEF's horizontal plane (see Fig. 5). In the case of undercutting, sweeping of the ram atomic oxygen in the horizontal plane due to the orbital inclination would cause a slightly higher fluence per angle of arrival than in the vertical plane, causing wider undercutting. It would also cause wider undercutting due to additional trapping of the scattered atomic oxygen within the undercut cavity. All these contributions (scattering, thermal velocity, and orbital inclination), combined with the LDEF's 8.1-deg yaw offset (ram misalignment),[8] result in a more complex interaction, and a correspondingly more complex atomic-oxygen erosion process, than the more simplistic result that one might expect of atomic oxygen arriving from only the fixed orbital orientation.

These atomic-oxygen velocity components, transverse to the ram direction, which contribute to direct ram undercutting of defect sites in protective coatings on the LDEF, will affect all LEO orbiting spacecraft. If a spacecraft system is solar-facing it will sweep in angle with respect to the ram direction. This will result in wider undercut cavities than those resulting from direct ram attack. Atomic-oxygen undercutting on spacecraft has not been previously documented due to the low fluence obtained on typical Shuttle exposures. The LDEF's high fluence provides one of the only opportunities to study LEO atomic-oxygen undercutting.

An aluminized-Kapton multilayer insulation (MLI) sample, which was located on the leading edge of the LDEF (row F-9), was used to study LEO direct ram atomic-oxygen undercutting.

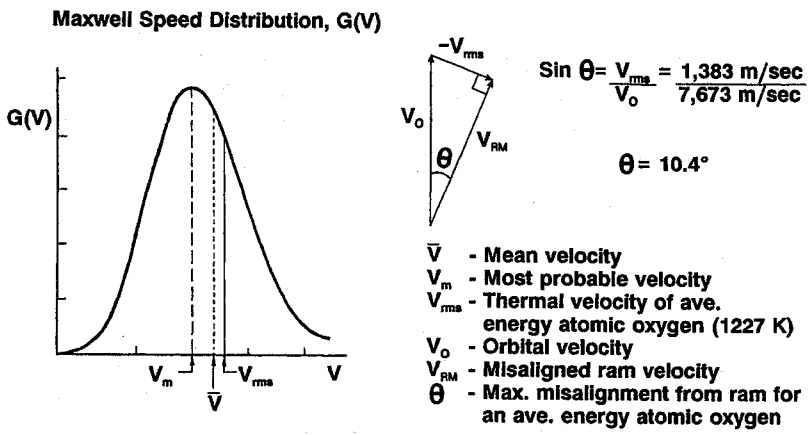

Fig. 2 Misalignment of ram atomic-oxygen impact due to thermal velocity contributions of randomly oriented hot thermospheric oxygen.

Undercut profiles were compared to Monte Carlo predictions of LEO ram atomic-oxygen undercut profiles. Dependencies in the undercut widths for various crack sizes, and whether the cracks were located in the vertical or horizontal planes of the LDEF, are presented. These results provide evidence of the complex interactions which LEO direct ram atomic oxygen can have on spacecraft, and the potentially damaging effect undercutting can have on vulnerable materials which have defected protective coatings.

Experimental Procedures

Material

The material evaluated in this study was an aluminized-Kapton multilayer insulation sample from the McDonnell Douglas Cascaded Variable Conductance Heat Pipe Experiment, Experiment A0076 (see Ref. 9 and Fig. 6). This sample was located on the leading edge of the LDEF, and was exposed to direct ram atomic oxygen. The Kapton was 0.0076 mm thick, with vent holes for depressurization purposes, and was aluminized (1000 Å) on both sides. The sample was launched with an exterior layer of 0.0762-mm-thick Kapton, containing no vent holes, and aluminized only on its unexposed side. This exterior layer was not present after retrieval of the LDEF except at the sample edges where the Kapton was attached underneath the experiment tray border. The exterior layer of Kapton would have been completely oxidized well before the retrieval of the LDEF, which should have caused loss of the unsupported aluminum, exposing the underlying protected MLI Kapton to direct ram atomic-oxygen exposure. The MLI sample analyzed was cut from an edge, and a section of protected exterior layer can be seen bent down in Fig. 6b. Only the top MLI layer which received direct ram exposure (where the exterior layer was missing) was analyzed.

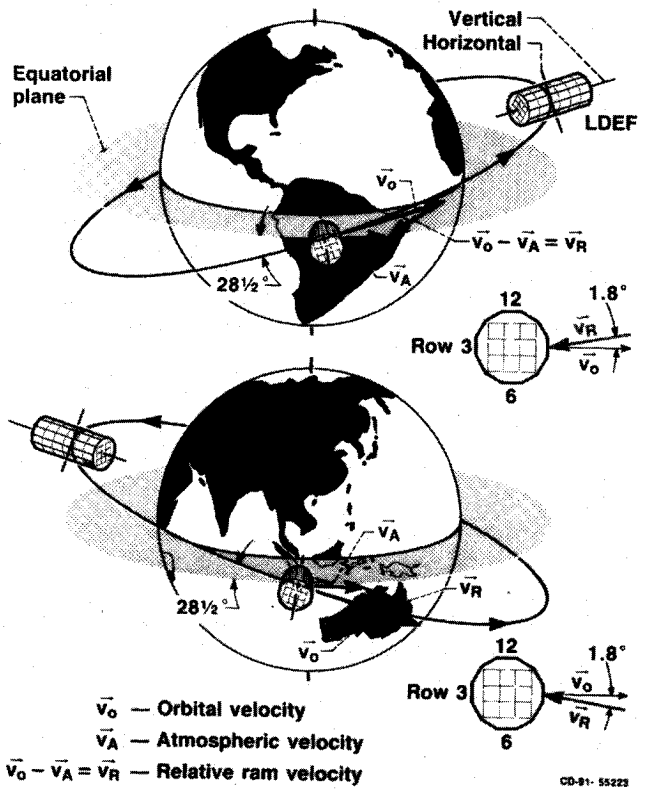

Fig. 3 Earth's atmospheric contribution to misalignment of ram atomic-oxygen impact on the LDEF.

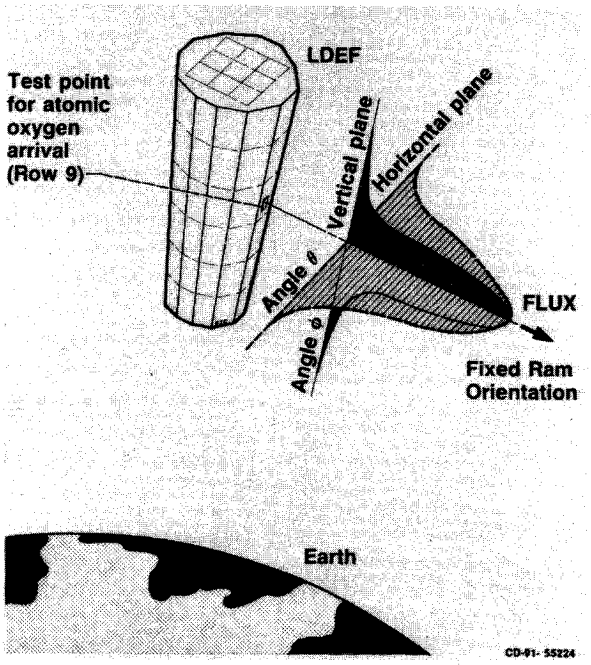

Fig. 4 Angular variation in atomic-oxygen flux on the LDEF due to the thermal and orbital inclination velocity contributions.

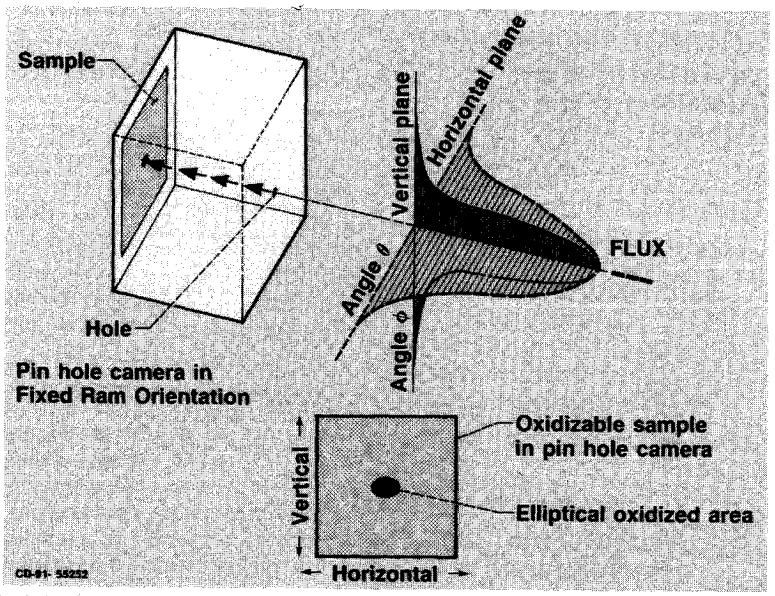

Fig. 5 Effect of the LDEF flux distribution variation in horizontal and vertical planes on pinhole camera samples.

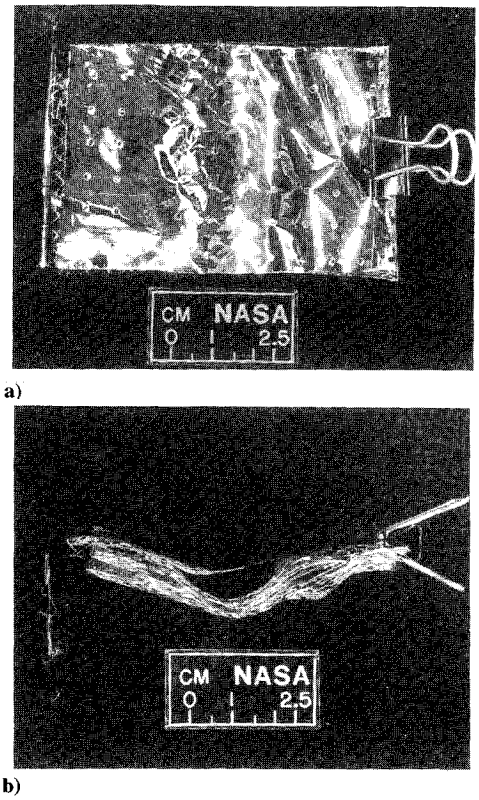

Fig. 6 Aluminized-Kapton multilayer insulation from the Cascaded Variable-Conductance Heat Pipe Experiment (A0076) located on row F-9: a) top view and b) side view.

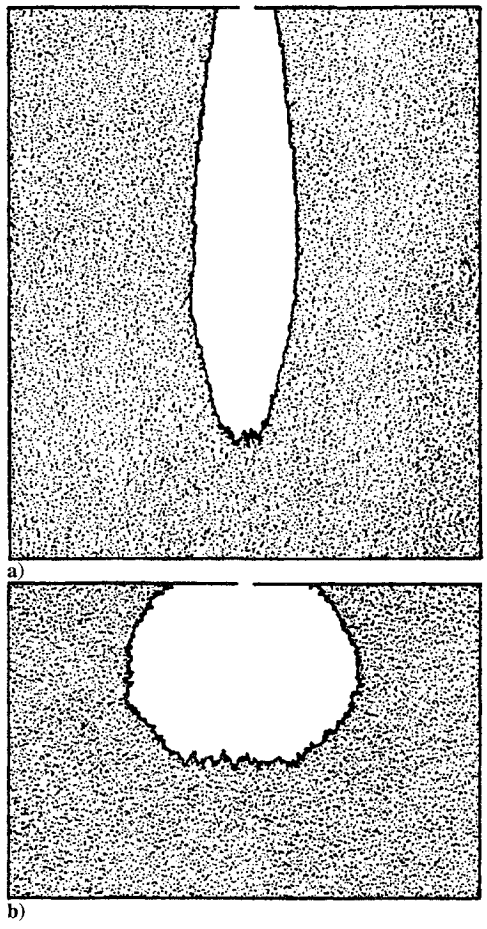

Fig. 7 Monte Carlo model atomic-oxygen undercutting predictions for protected Kapton in: a) normal incident space ram and b) sweeping space ram.

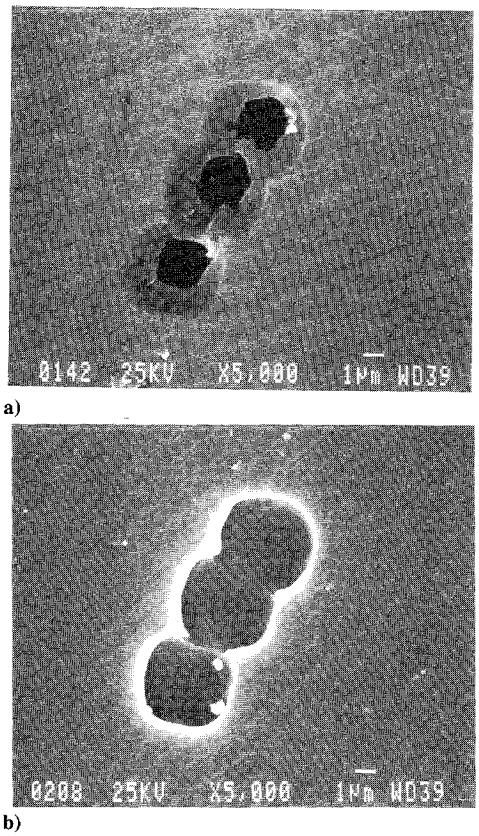

Fig. 8 Atomic-oxygen undercutting at pinhole defects on the LDEF aluminized-Kapton MLI: a) with aluminum and b) aluminum chemically removed revealing wide and shallow undercut cavities.

Fluence Exposure

The LDEF ram atomic-oxygen fluence for a 0-deg yaw offset has been determined to be 9.09×10^{21} atoms/cm^2 (see Ref. 8). Unfortunately, the LDEF was slightly misaligned about the yaw axis such that row 9 was not perpendicular to the velocity direction. Row 12 faced slightly into the ram direction and row 6 was tilted away from the ram direction. Misalignment of the surfaces from the velocity direction alters the atomic-oxygen fluence. Based on an average of four types of measurements, the LDEF yaw misorientation has been estimated to be 8.1 deg (see Ref. 8). The calculated fluence for row 9, at an 8.1-deg yaw offset from ram, has been determined to be 8.99×10^{21} atoms/cm^{21} (see Ref. 8).

Because the MLI sample was covered with a sheet of 0.0762-mm Kapton, the atomic-oxygen fluence of the MLI sample is calculated to be equal to the LDEF 8.1-deg yaw misalignment fluence for row 9, minus the fluence necessary to erode away the Kapton. The fluence necessary to erode the Kapton exterior sheet is equal to the thickness of the Kapton (0.0762 mm) divided by the erosion yield of Kapton. The erosion yield of Kapton at 8.1 deg off normal is the erosion yield for normal incidence multiplied by (cos 8.1 deg)$^{1/2}$ because the ram atomic-oxygen erosion yield of Kapton has been found to be dependent on $(\cos\Theta)^{1/2}$ (see Ref. 5) This fluence is calculated to be 2.55×10^{21} atoms/cm^2 An erosion yield of 3×10^{-24} cm^3/atom for Kapton was assumed based on previous space flight data.[10] The resulting atomic-oxygen fluence for the MLI sample is calculated to be 6.44×10^{21} atoms/cm^2.

Atomic-Oxygen Undercutting Evaluation

Small sections of the MLI sample were mounted, with the atomic-oxygen-exposed side up, onto aluminum scanning electron microscope (SEM) stubs using carbon paint. These samples

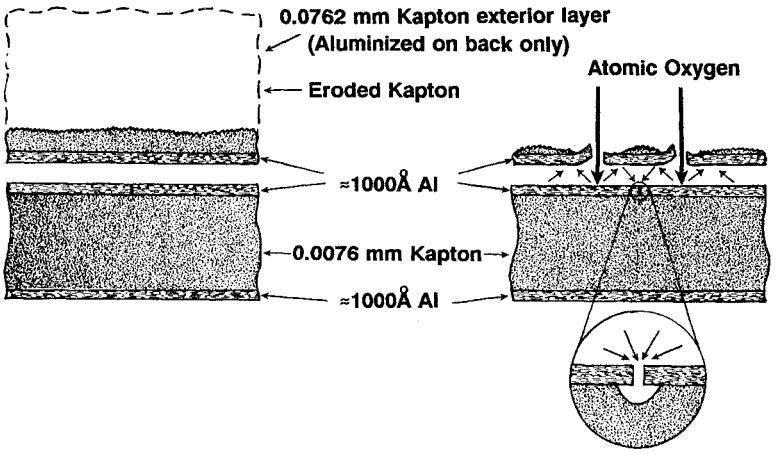

Fig. 9 Scattering of atomic oxygen due to crazing of the aluminized-Kapton exterior layer.

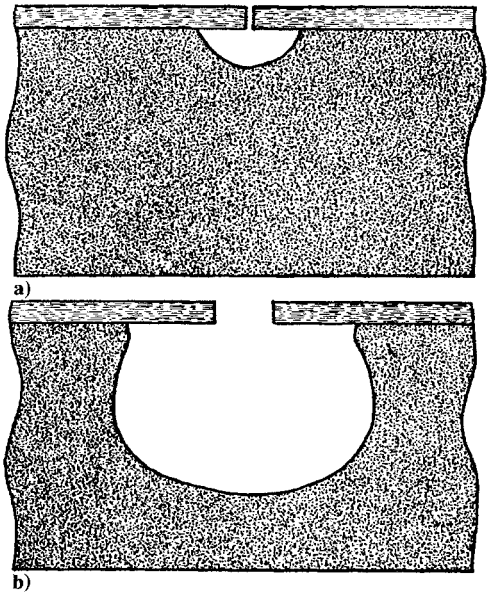

Fig. 10 Atomic-oxygen undercut profiles of the LDEF aluminized-Kapton: a) narrow cracks (<0.1 μm) and b) wide cracks (>0.1 μm).

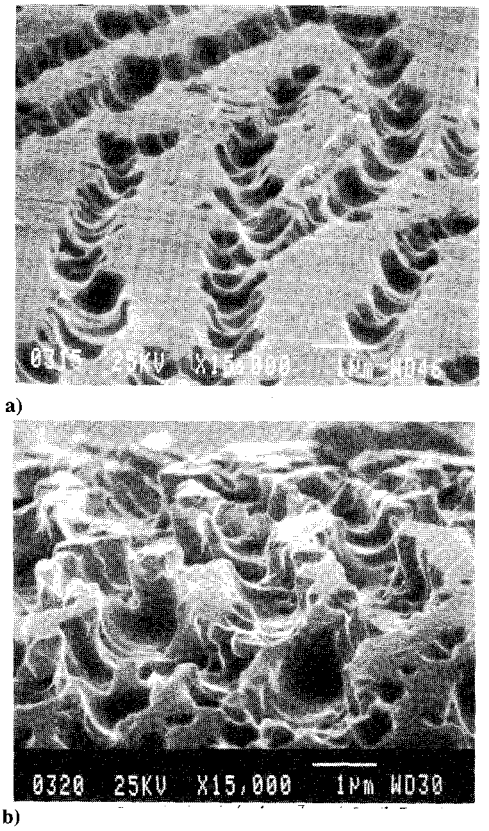

Fig. 11 Atomic-oxygen undercut profile images of the LDEF aluminized-Kapton: a) narrow cracks and b) wide cracks.

were then examined using a JEOL JSM-840A Scanning Microscope. Characteristic micrographs were taken of defect sites, including pinhole defects and microscopic cracks in the aluminization. Crack width measurements were obtained from electron micrographs of the aluminum-coated Kapton. Samples were then soaked in slightly diluted hydrochloric acid to remove the aluminum film. The samples were then remounted, coated with ≈150 Å of gold, and re-examined with the SEM. Identical locations were imaged so that defect widths could be directly compared with the undercut width. Undercut profile images of these areas were obtained by tilting samples, with the aluminum removed, at high tilt angles (60–75 deg).

Monte Carlo Model Comparisons

Predicted Monte Carlo undercut profiles are shown in Fig. 7 for normal incident space ram and sweeping space ram atomic-oxygen exposure conditions. The model predicts a narrower and deeper undercut cavity for normal incident space ram, and wider and shallower undercut cavity for sweeping space ram. Details of the Monte Carlo model are described in Ref. 5.

Results and Discussions

Examination of the MLI sample revealed wide and shallow undercutting at defect sites over 95% of the sample. Figure 8 shows undercutting at pinhole defects. The width of undercutting was extensive, and the depth very shallow, compared to Monte Carlo models for normal incident space ram. Therefore, an additional mechanism unique to this space experiment has been identified which appears to have contributed to undercutting. When the Kapton exterior layer was partially oxidized, cracks or holes probably developed in the exterior layer. Atomic oxygen then entered the holes and scattered around between the bottom of the aluminized exterior layer and the first MLI layer. This would cause a more isotropic arrival of atomic oxygen during the period of partial degradation of the exterior

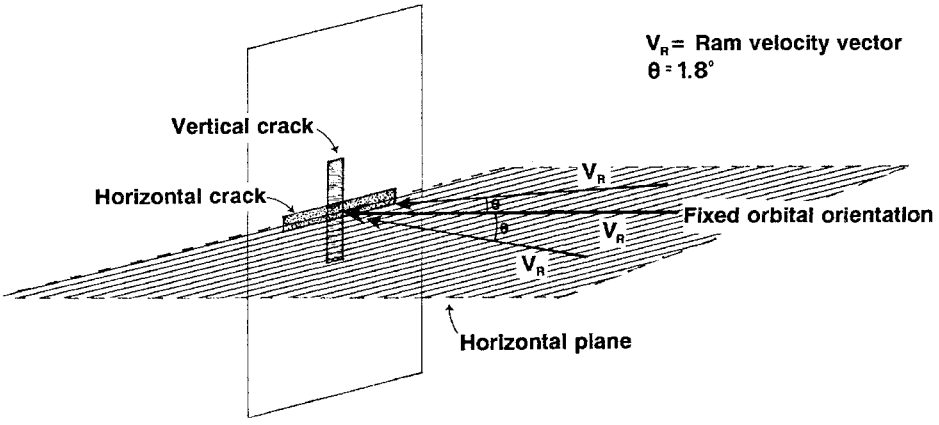

Fig. 12 Effect of orbital inclination on ram atomic-oxygen impact in the LDEF's horizontal and vertical planes; ram atomic oxygen swept parallel to horizontal cracks and perpendicular to vertical cracks.

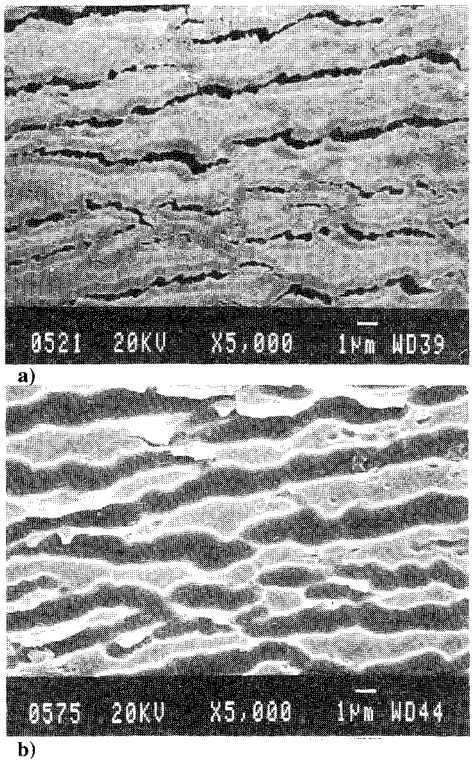

Fig. 13 Wide horizontal cracks in aluminized-Kapton MLI sample: a) with aluminum and b) aluminum chemically removed.

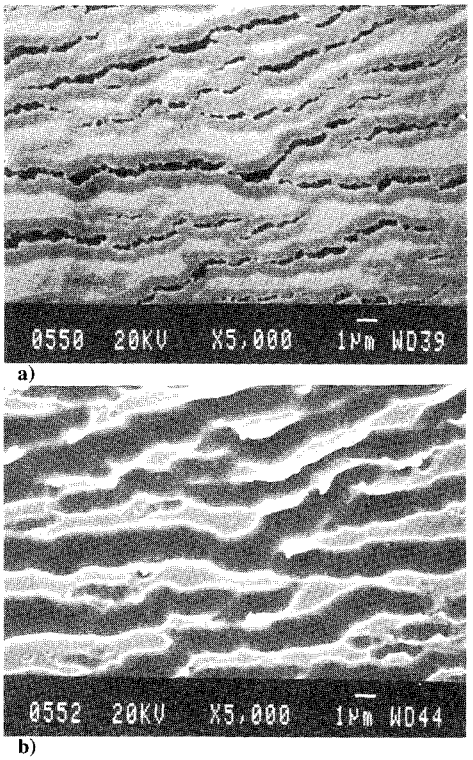

Fig. 14 Wide vertical cracks in aluminized-Kapton MLI sample: a) with aluminum and b) aluminum chemically removed.

layer than would be experienced during directed ram exposure. This scattering process is shown schematically in Fig. 9.

The size and shape of undercutting was found to vary with crack size, which is proportional to the number of oxygen atoms entering the defect. Narrower cracks were found to have U-shaped undercut profiles which were wider at the Kapton/aluminum interface than at the base of the profile. Wider cracks had more circular undercut regions, and the undercut profile was wider at the base than at the Kapton/aluminum interface. Figure 10 schematically shows the difference in undercut profiles for wide and narrow cracks, and Fig. 11 shows electron micrograph images of narrow and wide crack undercut profiles.

Because the ram atomic oxygen swept parallel to horizontal cracks and perpendicular to vertical cracks (see Fig. 12), it was expected that there would be a slight difference in the undercut profiles for vertical and horizontal cracks. The MLI sample was found to contain concentric cracks in the aluminization around the vent holes. These concentric cracks allowed a comparison between the undercut profiles of vertical and horizontal cracks. Figure 13 shows electron micrographs of wide horizontal cracks with and without the aluminum coating. Figure 14 shows electron micrographs of comparably wide vertical cracks with and without the aluminum coating. By tilting the sample with the aluminum removed, the undercut profiles for these horizontal and vertical cracks can be seen for wide cracks (see Fig. 15) and narrow cracks (see Fig. 16).

There are some distinct differences between the undercut profiles for horizontal and vertical cracks. The horizontal crack profiles are rounded at the base and have a very shallow pit burrowed in the bottom along the crack length. The vertical crack profiles are wider and smooth at the base. The variation in the undercut shapes may be possible because the directed atomic oxygen swept parallel to horizontal cracks (causing a deeper undercutting below the crack) and swept perpendicular to vertical cracks (causing a widening and smoothing effect), as seen in Fig. 17. The off center burrowed pits of the horizontal crack profiles and unsymmetric shape of the vertical crack profiles can be attributed to the 8.1-deg yaw offset. Figure 18 shows a plot of the difference in undercut widths for horizontal

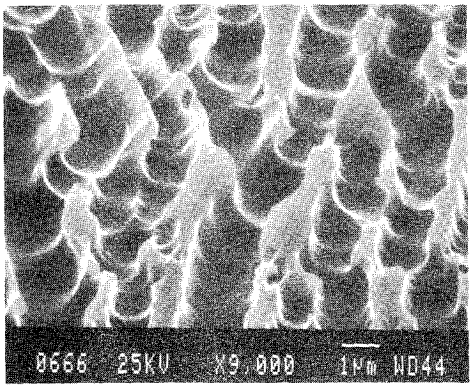

a)

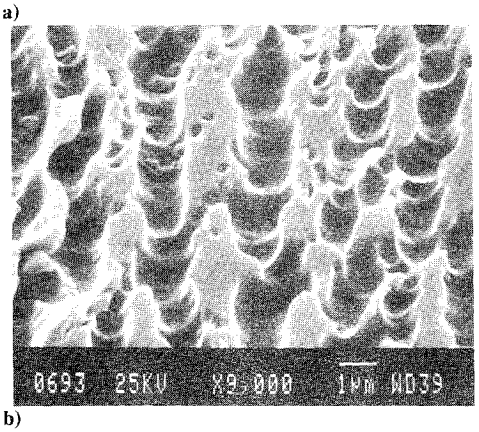

b)

Fig. 15 Wide cracks in aluminized-Kapton MLI sample: a) horizontal undercut profiles and b) vertical undercut profiles.

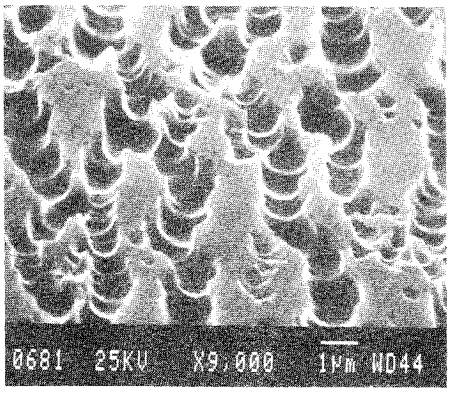

a)

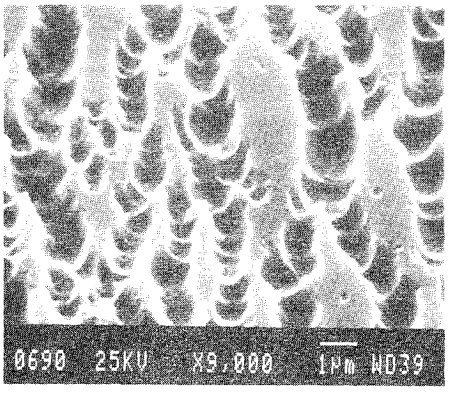

b)

Fig. 16 Narrow cracks in aluminized-Kapton MLI sample: a) horizontal undercut profiles and b) vertical undercut profiles.

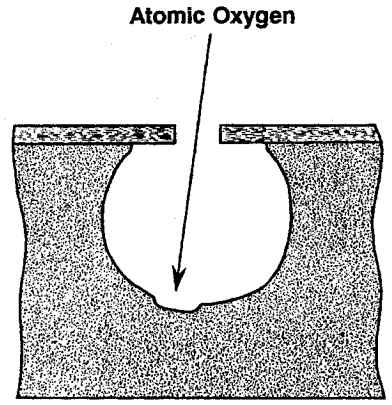

a)

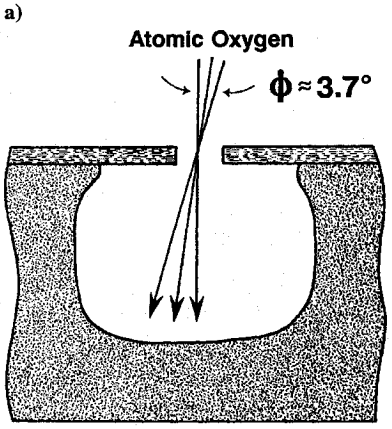

b)

Fig. 17 Variation in undercut profiles due to Earth's atmospheric contribution to ram impact misalignment: a) horizontal cracks (sweep was parallel to crack) and b) vertical cracks (sweep was perpendicular to crack).

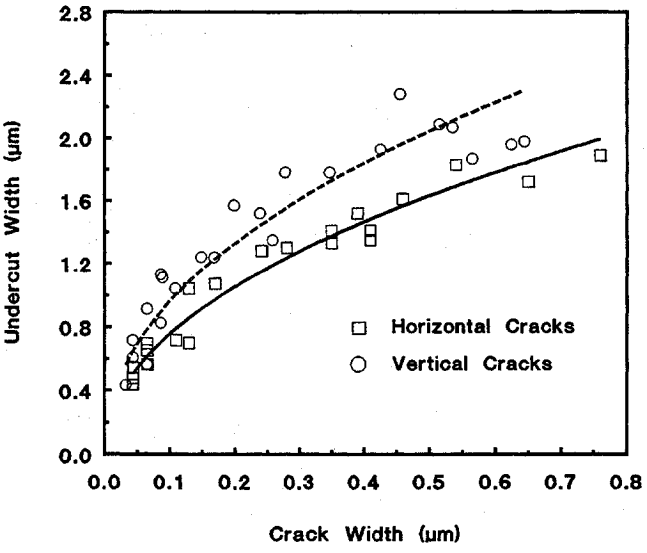

Fig. 18 LDEF aluminized-Kapton MLI: undercut width vs crack width.

and vertical cracks. Undercut widths exceeded crack widths by a factor of 2.5–12.5 for horizontal cracks, and 3.1–16.6 for vertical cracks. These undercut widths were measured at the Kapton/aluminum interface; however for wide cracks, the degree of undercutting was more severe because the base of the undercut profile was larger than at the measured interface.

Although the differences in the undercut widths are clear in Fig. 18, it is difficult to account quantitatively for the observed results. These difficulties arise from uncertainties in the exact fluence at which the aluminum exterior layer was lost and the extent to which undercutting resulted from atomic oxygen being

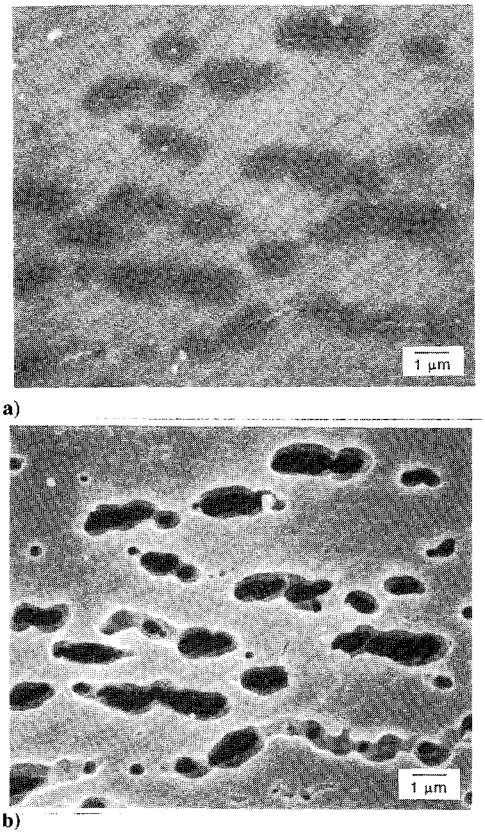

Fig. 19 Isolated area of cracks in aluminized-Kapton MLI sample with very deep undercut cavities: a) with aluminum and b) aluminum chemically removed.

scattered beneath the aluminum layer while it was still partially intact. However, preliminary calculations suggest that the atomic-oxygen angular flux distribution for vertical vs horizontal cracks, combined with the associated additional trapping of scattered atomic oxygen within vertical cracks, may be sufficient to account for a portion of undercutting differences. Nevertheless, this portion appears insufficient to account for the total difference in undercut volumes observed and additional mechanisms should be considered. A slight yaw oscillation in the LDEF orbit could contribute to the observed results. Analysis of a pinhole camera located on the LDEF's leading edge indicates evidence of a ±1-deg yaw oscillation in addition to the ±1.85-deg oscillation caused by the 28.5-deg orbital inclination.[11]

The shape of the undercut profiles over 95% of the sample appeared to more closely match the Monte Carlo prediction for sweeping space ram, indicating a primarily isotropic type of atomic-oxygen arrival as a result of scattering below the remains of the aluminum coating. Over less than 5% of the sample, the undercut profiles were very deep, and appear very similar to the Monte Carlo-predicted profile for normal incident space ram. Figure 18 shows an isolated location of crack defects, and the corresponding undercut images. It is believed that the depth of the undercut cavities at these defects sites may penetrate the 0.0076-mm thick Kapton.

The differences in undercut profiles between those observed over 95% of the sample (wide and shallow) and those predicted by the model (narrow and deep) indicate that the aluminization on the backside of the exterior layer of Kapton must have been crazed, or contained holes, but remained intact long after oxidative removal of the Kapton. Therefore, most of this MLI sample appears to have received isotropic atomic-oxygen arrival for the majority of the mission, resulting in wide, shallow undercutting, while a few isolated areas received normal incident atomic-oxygen arrival directly below holes in the exterior layer. The fact that this sample was cut from the experiment edge where protected exterior layer material was still intact increases the possibility of maintaining the aluminization over this section of MLI for a period of time after Kapton removal. The aluminization of the exterior layer appears to have eventually disintegrated, which allowed a short duration of direct ram exposure, thus providing the differences in horizontal and vertical cracks, as were seen.

Evaluation of direct ram undercutting of a protected graphite epoxy coupon, also located on the leading edge of the LDEF (with no exterior layer), provided evidence of deep undercutting at all coating defect sites, as expected for direct space ram attack.[12] This further confirms our conclusion that the bottom surface aluminization of the MLI exterior layer remained intact for a period of time after the unprotected Kapton was completely removed by oxidation. Details of the undercutting evaluation of the graphite epoxy sample and modification to the Monte Carlo model based on these results are given in Ref. 12.

Conclusions

Explanations for atomic-oxygen undercutting of protected oxidizable materials exposed to direct (normal incident) space ram atomic oxygen in LEO are given. A section of aluminized-Kapton MLI sample exposed on the leading edge of the LDEF was evaluated for direct ram atomic-oxygen undercutting. The MLI Kapton exterior layer (aluminized only on the back side), not present after LDEF retrieval, was expected to have been completely eroded after a fluence of 2.55×10^{21} atoms/cm^2, exposing the underlying MLI sample to a fluence of 6.44×10^{21} atoms/cm^2. Evaluation of the undercut profiles for 95% of the MLI sample reveal much wider and shallower undercut cavities than predicted by Monte Carlo modeling for normal incident space ram. This indicates that the aluminization of the exterior layer over this sample must have remained intact, but crazed, after removal of the Kapton layer. This resulted in isotropic arrival of atomic oxygen during the majority of the mission. Differences between horizontal and vertical cracks were observed which might have resulted during a short exposure to direct ram atomic-oxygen attack when the aluminum film finally disintegrated. A yaw instability would have helped to exaggerate the differences observed. A few isolated areas experienced very deep undercut cavities, as predicted by Monte Carlo modeling. These areas appeared to have received direct ram exposure at holes in the exterior layer. Evaluation of this sample has provided evidence of atomic-oxygen undercutting for directed and scattered LEO atomic-oxygen attack. These results help emphasize the complex nature, and potential degrading effects, of LEO atomic-oxygen erosion.

Acknowledgments

The authors would like to thank Timothy McCollum for his contributions to the understanding of potential undercutting differences in vertical and horizontal cracks.

References

[1] Gulino, D. A., "Space Station Solar Concentrator Materials Research," NASA TM-100862, May 1988.

[2] Anon., U.S. Standard Atmosphere, 1976, U.S. Government Printing Office, Washington, DC, 1976, p. 30.

[3] Rutledge, S. K., and Mihelcic, J. A., "Undercutting of Defects in Thin Film Protective Coatings on Polymer Surfaces Exposed to Atomic Oxygen," NASA TM-101986, April 1989.

[4] de Groh, K. K., Terlep, J. A., and Dever, T. M., "Atomic Oxygen Durability of Solar Concentrator Materials for Space Station Freedom," *Proceedings from the 5th Annual Air Force Workshop on Surface Reactions in the Space Environment*, Northwestern University, Evanston, IL, Sept. 1990.

[5] Banks, B. A., Auer, B. M., Rutledge, S. K., and Hill, C. M., "Atomic Oxygen Interaction with Solar Array Blankets at Protective Coating Defect Sites," *4th Annual Workshop on Space Operations Applications and Research (SOAR '90)*, NASA CP-3103, Vol. II, June 1990, pp. 726–732.

[6] Banks, B. A., Rutledge, S. K., Auer, B. M., and DiFilippo, F., "Atomic Oxygen Undercutting of Defects on SiO_2 Protected Polyimide

Solar Array Blankets," *Materials Degradation in Low Earth Orbit (LEO)*, The Minerals, Metals & Materials Society, Warrendale, PA, 1990, pp. 15–33.

[7]Bourassa, R. J., and Gillis, J. R. "Atomic Oxygen Exposure of LDEF Experiment Trays," NASA CR-189627, May 1992.

[8]Stein, B., "LDEF Materials Overview," *LDEF — 69 Months in Space, Second Post-Retrieval Symposium*, NASA CP-3194, Part 3, June 1992, pp. 741–789.

[9]Grote, M. G., and Calhoun, L. D., II, "Cascade Variable-Conductance Heat Pipe (A0076)," *The Long Duration Exposure Facility (LDEF) Mission 1 Experiments*, NASA SP-473, Feb. 1984, pp. 66–69.

[10]Leger, L. J., and Visentine, J. T., "A Consideration of Atomic Oxygen Interactions with the Space Station," *Journal of Spacecraft and Rockets*, Vol. 23, No. 5, 1986, pp. 505–511.

[11]Palmer, P. N., Whitehouse, P. L., and Gregory, J. C., "Refinements on the Pinhole Camera Measurements of the LDEF Attitude," *LDEF—69 Months in Space, Second Post-Retrieval Symposium*, NASA CP-3194, Part 1, June 1992, pp. 3–12.

[12]Banks, B. A., de Groh, K. K., Auer, B. M., Gebauer, L., and Edwards, J. L., "Monte Carlo Modeling of Atomic Oxygen Attack of Polymers with Protective Coatings on LDEF," *LDEF—69 Months in Space, Second Post-Retrieval Symposium*, NASA CP-3194, Part 3, June 1992, pp. 1137–1150.

Ronald K. Clark
Associate Editor